REPRODUCTION
RESEARCH

Lamin A/C proteins in the spermatid acroplaxome are essential in mouse spermiogenesis

Jian Shen*, Wen Chen*, Binbin Shao*, Yujuan Qi, Zhengrong Xia, Fuqiang Wang, Lei Wang, Xuejiang Guo, Xiaoyan Huang and Jiahao Sha

State Key Laboratory of Reproductive Medicine, Department of Histology and Embryology, Nanjing Medical University, 140 Hanzhong Road, Nanjing, Jiangsu Province 210029, People's Republic of China

Correspondence should be addressed to X Guo; Email: guo_xuejiang@njmu.edu.cn or to be X Huang; Email: bbhxy@njmu.edu.cn

*(J Shen, W Chen and B Shao contributed equally to this work)

Abstract

Spermiogenesis is a complex process of terminal differentiation that is necessary to produce mature sperm. Using protein expression profiles of mouse and human testes generated from our previous studies, we chose to examine the actions of lamin A/C in the current investigation. Lamin A and lamin C are isoforms of the A-type lamins that are encoded by the *LMNA* gene. Our results showed that lamin A/C was expressed in the mouse testis throughout the different stages of spermatogenesis and in mature sperm. Lamin A/C was also expressed in mouse haploid germ cells and was found to be localized to the acroplaxome in spermiogenesis, from round spermatids until mature spermatozoa. The decreased expression of lamin A/C following injections of siRNA against *Lmna* caused a significant increase in caudal sperm head abnormalities when compared with negative controls. These abnormalities were characterized by increased fragmentation of the acrosome and abnormal vesicles, which failed to fuse to the developing acrosome. This fragmentation also caused significant alterations in nuclear elongation and acrosome formation. Furthermore, we found that lamin A/C interacted with the microtubule plus-end-tracking protein CLIP170. These results suggest that lamin A/C is critical for proper structural and functional development of the sperm acrosome and head shape.

Reproduction (2014) **148** 479–487

Introduction

To generate mature spermatozoa, germ cells undergo mitosis (self-renewal and proliferation of spermatogonia), meiosis (generation of round spermatids), and spermiogenesis (transformation of round spermatids into sperm) (Eddy 2002, Sha *et al*. 2002). Spermiogenesis is a unique process that involves the formation of an acrosome and the sperm tail, elongation and condensation of the nucleus, and removal of unnecessary cytoplasm. The acrosome is a membranous apparatus that forms through an integrated process in the production of transport vesicle, trafficking, and fusion. During this process, Golgi-derived pro-acrosomal vesicles attach to and align along the acroplaxome. The acroplaxome is a plate found in the subacrosomal space that consists of F-actin and keratin, and is anchored to the developing acrosomes in the nuclei of elongating spermatids (Kierszenbaum *et al*. 2003, Kierszenbaum & Tres 2004).

In our previous studies, we used different proteomic technologies to determine protein expression of whole mouse and human testes (Zhu *et al*. 2006, Huang *et al*. 2008, Guo *et al*. 2010*a*, Liu *et al*. 2013). We reported protein expression of germ cells at different developmental stages, including meiotic and haploid germ cells, thereby identifying the proteomic profiles of cells associated with spermatogenesis (Guo *et al*. 2010*b*, 2011). These data have helped to develop our understanding of the regulation of male fertility (Huang & Sha 2011). Several proteins reported in these studies were selected for further investigation.

Lamin A/C belongs to A-type lamins and is derived by differential splicing from the *LMNA* gene. A-type lamins are components of the nuclear envelope and are primarily expressed in well-differentiated cells. It has been suggested that A-type lamins are involved in the terminal differentiation of cells (Collard *et al*. 1992, Genschel & Schmidt 2000, Galiová *et al*. 2008). Mutation in the *LMNA* gene appears to be responsible for several inherited disorders in humans, including Emery–Dreifuss muscular dystrophy (EDMD), Dunnigan-type familial partial lipodystrophy (FPLD), and Hutchinson–Gilford progeria syndrome (Worman &

ISSN 1470–1626 (paper) 1741–7899 (online)
DOI: 10.1530/REP-14-0012
Online version via www.reproduction-online.org

Courvalin 2004, 2005). In addition, the disruption of *Lmna* activity causes male infertility as a result of impaired spermatogenesis. In spermatocytes, the depletion of lamin A/C causes defective synaptic pairing of the sex chromosomes, which prevents the completion of meiosis and leads to increased apoptosis during the late-pachytene stage of meiosis I (Alsheimer *et al*. 2004). However $Lmna^{-/-}$ mice actually lack the expression of both meiosis-specific lamin C2 and somatic A-type lamins A and C and, as a consequence, show a strong somatic disease phenotype. Then a lamin C2 isoform-specific knockout model was generated and the results demonstrate that lamin C2 contributes directly to fertility through facilitation of meiotic chromosome movements (Link *et al*. 2013). Due to incomplete meiosis, $Lmna^{-/-}$ mice are unable to generate haploid spermatids. The detailed biological significance of lamin A/C during spermiogenesis is largely unknown.

In this study, we report that lamin A/C was also expressed in mouse haploid germ cells and specifically localized to acroplaxome in spermiogenesis, from round spermatids until mature spermatozoa. The decreased expression of lamin A/C following injection of siRNA against *Lmna* caused a significant increase in cauda sperm head abnormalities. Furthermore, our data suggest that lamin A/C interacts with CLIP170, a manchette-associated protein involved in shaping sperm head.

Materials and methods

Animals

ICR mice were maintained under a controlled environment of 20–22 °C, with a 12 h light:12 h darkness cycle, 50–70% humidity, and food and water *ad libitum*. Before sample collection, approval was granted for the study protocol by the Animal Research Committee of Nanjing Medical University.

Sample preparation and protein extraction

By using the standard swim up technique, 0d, 7d, 14d, 21d, 28d, and 60d testis samples and caudal epididymal sperm from adult epididymis were collected from ICR mice. From 3-week-old and adult ICR mice, respectively, 4C and 1C mouse germ cells (where C=haploid DNA content) were sorted via flow cytometry as described previously (Guo *et al*. 2010*b*, 2011). From 3-week-old ICR mice, spermagonia, secondary spermatocytes, and somatic cells with 2C DNA contents were sorted as 2C cells. The samples were solubilized in lysis buffer (7 M urea, 2 M thiourea, 4% (w/v) CHAPS, 2% (w/v) dithiothreitol) in the presence of 1% (v/w) protease inhibitor cocktail (Pierce Biotechnology, Rockford, IL, USA). The testes were homogenized while caudal sperm were sonicated, and placed on a shaker at 4 °C for 1 h. The insoluble matter was subsequently removed by centrifugation at 40 000 ***g*** at 4 °C for 1 h. The protein concentration in each sample was determined by the Bradford method, using BSA as the standard.

Western blotting analysis

The samples containing 100 μg protein were electrophoresed a 12% SDS–polyacrylamide gel and transferred to a polyvinylidene fluoride membrane (GE Healthcare, Milwaukee, WI, USA). The membranes were blocked in TBS containing 5% nonfat milk powder for 1 h and then incubated overnight with anti-lamin A/C polyclonal antibody (1:1000, Cat No. #2032, Cell Signaling Technology, Boston, MA, USA) and anti-β-tubulin polyclonal antibody (1:2000, Abcam, Cambridge, MA, USA) diluted in TBS and 5% nonfat milk powder. The expression of β-tubulin was used as a loading control. The membranes were washed and then incubated for 1 h with HRP-conjugated goat anti-rabbit IgG (1:1000, Beijing ZhongShan Biotechnology Co., Beijing, China). Specific proteins were detected using an ECL kit and AlphaImager (GE Healthcare Bio-Sciences Corp., Piscataway, NJ, USA).

Indirect immunofluorescence

The testis tissue was embedded in optimal cutting temperature (OCT) compound, cryosectioned into 5 μm thick sections (CM1900, Leica Microsystems, Wetzlar, Germany), mounted on slides, and then left to dry before fixation. A single-cell suspension from the testis tissue was prepared by using the Medimachine (BD Biosciences, San Jose, CA, USA). The sperm collected from the testis or cauda epididymis were then air-dried onto slides. The slides prepared were fixed with 4% formaldehyde in PBS for 30 min, washed with PBS, and then blocked with goat serum (Beijing ZhongShan Biotechnology Co.) for 2 h at room temperature. Following incubation with primary antibodies (lamin A/C, 1:100, Cell Signaling Technology) overnight at 4 °C, the cells were incubated with a FITC-labeled secondary antibody (Beijing ZhongShan Biotechnology Co.) at a dilution of 1:200 for 1 h at room temperature. Normal rabbit IgG was used as a primary antibody in the negative-control condition (Santa Cruz Biotechnology). The nucleus was stained with 5 μg/ml Hoechst H33342 (Sigma–Aldrich) for 30 s. All samples were observed under a ZEISS LSM 710 confocal microscope (Carl Zeiss, Oberkochen, Germany).

Double immunofluorescence of precapacitated sperm and testis single cell

For the double-immunofluorescence procedure, in addition to the same methods aforementioned for the indirect immunofluorescence, a second antibody labeled with tetraethyl rhodamine isothiocyanate (TRITC) was used (Beijing ZhongShan Biotechnology Co.). The slides were placed in 30 μg/ml of FITC-labeled *Pisum sativum* agglutinin (PSA, Sigma) for 1 h for acrosome staining at room temperature. To determine F-actin staining, the slides with lamin A/C-stained sperm were placed in 5 μg/ml TRITC-labeled phalloidin (Sigma–Aldrich) for 1 h at room temperature. The nucleus was stained with 5 μg/ml Hoechst H33342 (Sigma–Aldrich) for 30 s. Normal rabbit IgG was used as a primary antibody in the negative-control condition (Santa Cruz Biotechnology). All samples were observed under a ZEISS LSM 710 (Carl Zeiss).

Intratesticular injection of siRNA against Lmna

SiRNAs against *Lmna* mRNA (Invitrogen) were diluted to a final concentration of 20 μM and stored at −20 °C. The efficiencies of the three siRNAs were verified using the GC-2spd (ts) cell line (ATCC, Manassas, VA, USA), as per manufacturer's instructions. Nine 3-week-old male mice (three for 48 h analysis, three for 72 h analysis, and three for final epididymal sperm morphology analysis) were anesthetized with sodium pentobarbital and the testes were exteriorized through a 5 mm midline abdominal incision. For each mouse, ∼3–5 μl of siRNA mixed with 0.4% trypan blue was injected into one testis through the rete testis, as described previously (Ikawa *et al*. 2002, Lu *et al*. 2006, Qi *et al*. 2013). The other testis was injected with negative-control siRNA (Invitrogen). After the injection, testes were replaced and the abdomen was sutured. The mice were allowed to recover and were left undisturbed until analysis. At both 48 and 72 h following the siRNA injection, a subset of animals were killed, testes removed and processed for western blotting analysis to determine the relative changes in protein expression between groups. To analyze the results of western blotting, Image J software was used to quantify protein bands via densitometry. The subsequent *in vivo* RNA interference analysis was performed at the same condition.

Epididymal sperm morphology classification

Three weeks following the siRNA injection, spermatozoa were collected from the cauda epididymis, spread onto slides, fixed with 4% PFA, and stained using hematoxylin and eosin (HE) or PSA (as described earlier) for morphological observation. Sperm deformities were classified as described previously (Davis & Gravance 1994) and classified as two types: sperm head abnormality and sperm tail abnormality. Three hundred sperm were counted in each slide by a double-blind method.

Statistical analyses

Statistical differences between two groups were measured by Student's *t*-test with $P<0.05$ considered to be significant.

Transmission electron microscopy

For ultra structural examination, spermatozoa collected from the cauda epididymis were first fixed in 4% glutaraldehyde, then postfixed with 2% OsO_4, and finally embedded in Araldite. Ultrathin sections (50 nm) stained with uranyl acetate and lead citrate were observed using an electron microscope (JEM.1010, JEOL, Tokyo, Japan).

Immunoprecipitation

Co-immunoprecipitation (Co-IP) was carried out as per the manufacturer's instructions (Sigma–Aldrich). Briefly, the testes were lysed in RIPA buffer (50 mM Tris–HCl (pH 7.5), 150 mM NaCl, 1% (v/v) NP-40, 0.1% (w/v) SDS, 1% (w/v) sodium deoxycholate) in the presence of a 1% (v/w) protease inhibitor cocktail. The supernatant was then incubated with rabbit anti-lamin A/C polyclonal antibody at 4 °C overnight. Normal rabbit IgG antibody was used as a control. The immunocomplex was then pulled down by Protein G-sepharose (Invitrogen). The resin was washed, eluted with SDS sample buffer, analyzed by SDS–PAGE, and immunoblotted with primary antibodies followed by HRP-coupled secondary antibodies. The gel was visualized using Coomassie Brilliant Blue (G250) staining and identified by MALDI-TOF/TOF as described previously (Wang *et al*. 2005).

Results

Expression and localization of lamin A/C during mouse spermatogenesis

To detect the expression levels of lamin A/C during mouse spermatogenesis, western blotting analysis was carried out using total mouse testis, sperm, and isolated testicular cells. As shown in Fig. 1A and B, there were two bands at the position of the expected molecular mass (70 and 65 kDa) in mouse testis at different developmental stages and sperm, which was concordant with the theoretical molecular weight of lamin A/C. To further clarify which type of germ cells show higher expression of lamin A/C, cells such as 4C, 1C germ cells and 2C cells (including spermagonia, secondary spermatocytes, and somatic cells) were isolated. Figure 1C shows high expression of lamin A/C in 2C cells and 1C germ cells.

High levels of lamin A/C expression were found in spermatids, as revealed by immunofluorescence analysis (Fig. 2A). The triple immunofluorescence of PSA, lamin A/C, and Hoechst showed that lamin A/C was positioned on the perinuclear region of the spermatids (Fig. 2C).

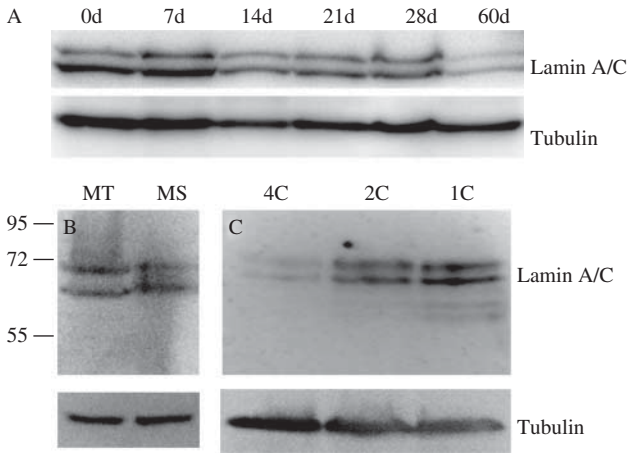

Figure 1 (A) Western blotting analysis showing the expression of lamin A (upper band) and C (lower band) in mouse testis at different developmental stage. (B) The expression of lamin A/C and tubulin in adult mouse testis (MT) and sperm (MS). (C) The expression of lamin A/C in testicular 4C, 1C germ cells, and 2C cells. Anti-β-tubulin was used as a loading control.

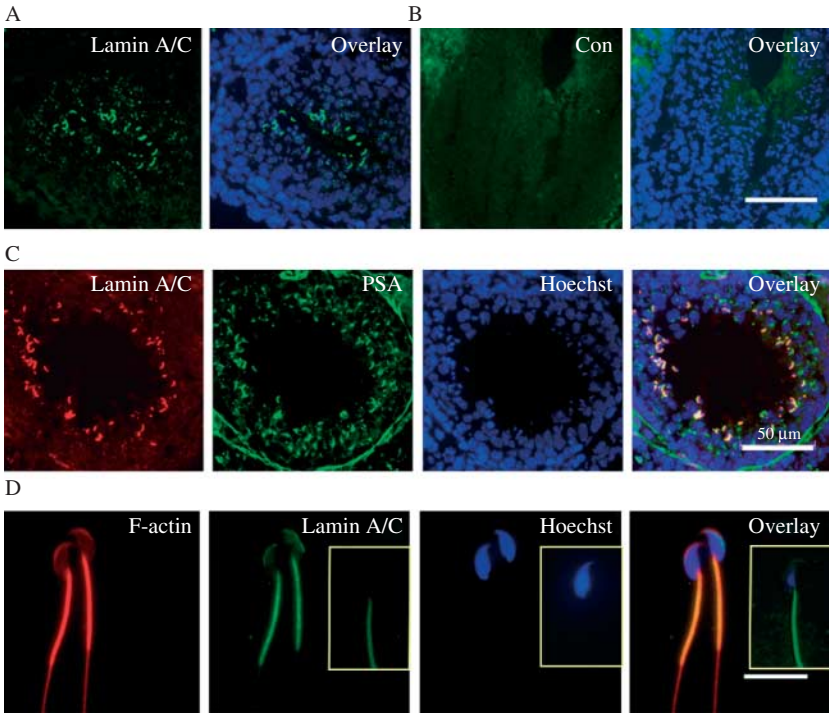

Figure 2 (A and B) Immunofluorescence staining of lamin A/C in mouse testis. Lamin A/C (green) was highly expressed in spermatids. The background staining of normal rabbit IgG was low (bar = 50 μm). (C) The co-localization of lamin A/C (red) and PSA (green). Lamin A/C was mainly localized in the perinuclear region of the spermatids (bar = 50 μm). (D) Lamin A/C (green) co-localized with F-actin (red) on sperm heads (bar = 10 μm). All the nuclei were stained with Hoechst (blue). The small yellow boxes in the right of lamin A/C, Hoechst stained and Overlay were indicated as negative control without primary antibody.

Subcellular localization of lamin A/C during mouse spermiogenesis

Lamin A/C was concentrated in the perinuclear region between nucleus and PSA, an established marker of the acrosome. The localization of lamin A/C changed with acrosome formation (Fig. 3). Following triple-immunofluorescence staining of nuclear, lamin A/C, and F-actin, we detected that lamin A/C was co-localized with F-actin in the mouse sperm head (Fig. 2D).

Lmna knockdown mice showed defects in nucleus and acrosome formation

The siRNA (Lmna-MSS205989, sense: UUUAGGGUGAACUUCGGUGGGAAGC; antisense: GCUUCCCACCGAAGUUCACCCUAAA) with highest protein inhibition efficiency 48 h after transfection in the GC2 cell line was used for subsequent analyses. Approximately, 30% of the seminiferous tubules were introduced with siRNA (Fig. 4A). The lamin A/C proteins were observed to be significantly suppressed in testis 48 and 72 h after siRNA injection (Fig. 4B and C). Lamin A was reduced by ∼50% and lamin C by about 60%.

Three weeks following siRNA injections, sperm from the caudal epididymis were collected for morphological analysis and 600–800 sperm were counted in each slide using a double-blind method. A large number of sperm from the cauda epididymides in mice treated with siRNA had abnormal heads that resembled irregularly shaped balls. The sperm from the negative-control group showed no such abnormalities (Fig. 4D, E, and F). Nearly 33% of sperm from testes treated with siRNA were abnormal, compared with 10% in the negative-control group ($P<0.01$). In the RNAi group, a significant increase in sperm head defects was observed, with ∼28% showing defects compared with only rare abnormalities in the negative-control groups ($P<0.01$) (Fig. 5A). These defects were clearly observed following the triple immunostaining of lamin A/C, PSA, and Hoechst respectively. Sperm with reduced expression of lamin A/C from the RNAi group was found to have abnormal acrosome stained. And the acrosomes failed to acquire the typical crescent moon shape and were found to be deformed and fragmented (Fig. 5B).

Results of the electron microscopic analysis showed that control sperm had elongated and condensed nuclei and one intact acrosome covering the nucleus (Fig. 6A). In mouse testes treated with siRNA against *Lmna*, the sperm were found to have deformed nuclei with abnormal acrosomes, fragmented and discrete acrosome vesicles, missing acrosomes, or abnormal arrangements of mitochondria in the mitochondrial sheath. In addition, all nuclei were malformed with a round or ovoid morphology. Occasionally, vacuole formation or invagination that gave the nucleus a crescent-shaped structure was also apparent (Fig. 6B, C, D, E, F, G, H, and I).

The lamin A/C protein interact with CLIP170

Compared with the normal rabbit IgG, immunoprecipitation with lamin A/C antibody pulled down a specific protein (about 170 kDa). Mass spectrometry

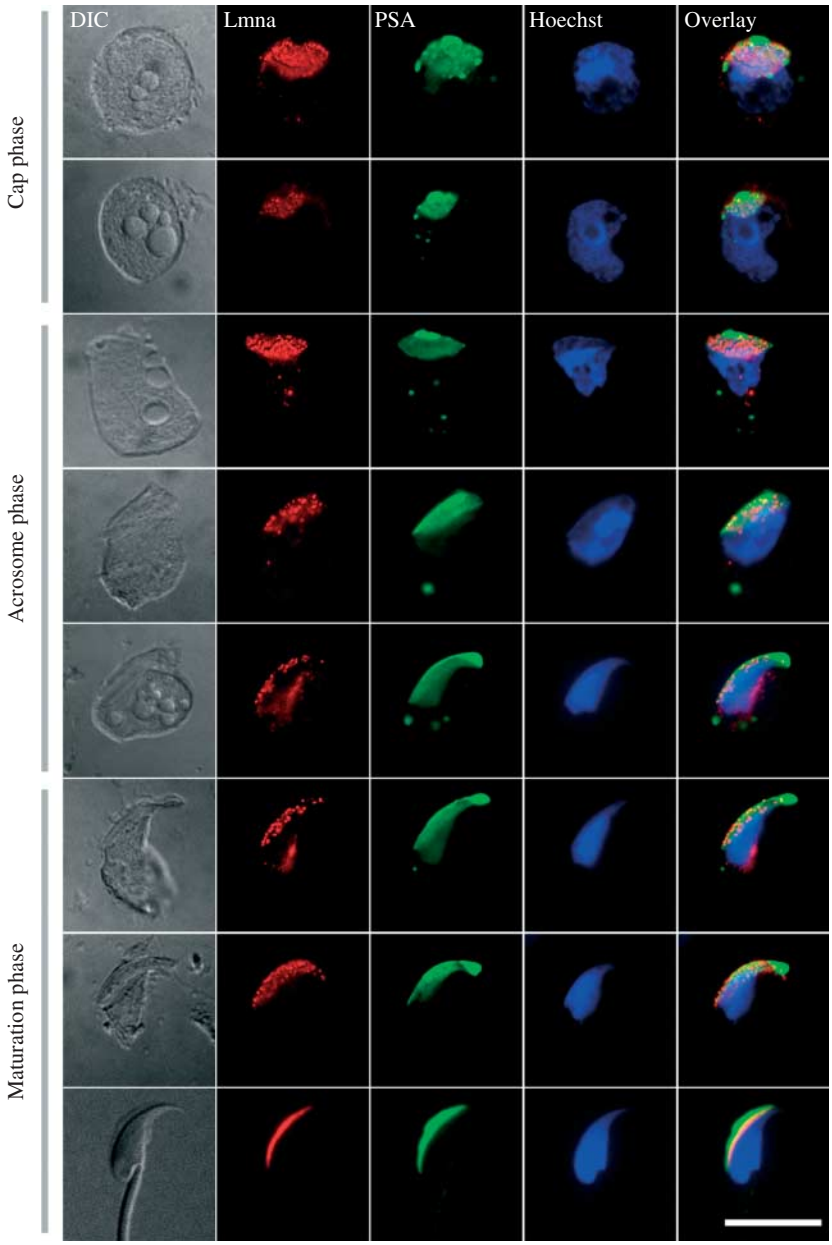

Figure 3 The co-localization of lamin A/C and PSA in different stages of spermatid from mouse testis was visualized by immunofluorescence. DIC (grey) indicated the morphology of different stages of spermatids. PSA (green) marked the acrosome of spermatid, and the nucleus was stained by Hoechst (blue). Lamin A/C (red) was consistently expressed between the acrosome and nucleus of spermatids during head elongation (bar = 10 μm).

identified that protein as CLIP170 (Fig. 7A), a manchette-associated protein, in developing spermatids (Akhmanova *et al.* 2005). The interaction between lamin A/C and CLIP170 was further confirmed by Co-IP from mouse testis. Lamin A/C was detected by immunoblotting in immunoprecipitated proteins obtained with anti-CLIP170 antibody from normal mouse testis extract (Fig. 7B).

Discussion

We identified numerous proteins related to mouse and human spermatogenesis in our recent work. Lamin A/C was first identified in the mouse testis proteome profile and was found to be involved in the first wave of spermatogenesis (Huang *et al.* 2008). Subsequently, lamin A/C was also identified in proteome profiles of human testes and sperm (Liu *et al.* 2013, Wang *et al.* 2013). The work done by Alsheimer *et al.* (2004) showed that Lmna$^{-/-}$ mice had a dramatic increase in apoptosis during late-pachytene stage and a breakdown of spermatogenesis. However, the function of lamin A/C during mouse spermiogenesis remained unknown. In the current investigation, we highlighted the functions of lamin A/C during mouse spermatogenesis.

The high level of lamin A/C expression observed in 1C germ cells suggests that these proteins tend to be expressed in haploid spermatids. Furthermore, immunolocalization studies showed lamin A/C was predominantly localized in spermatids and throughout

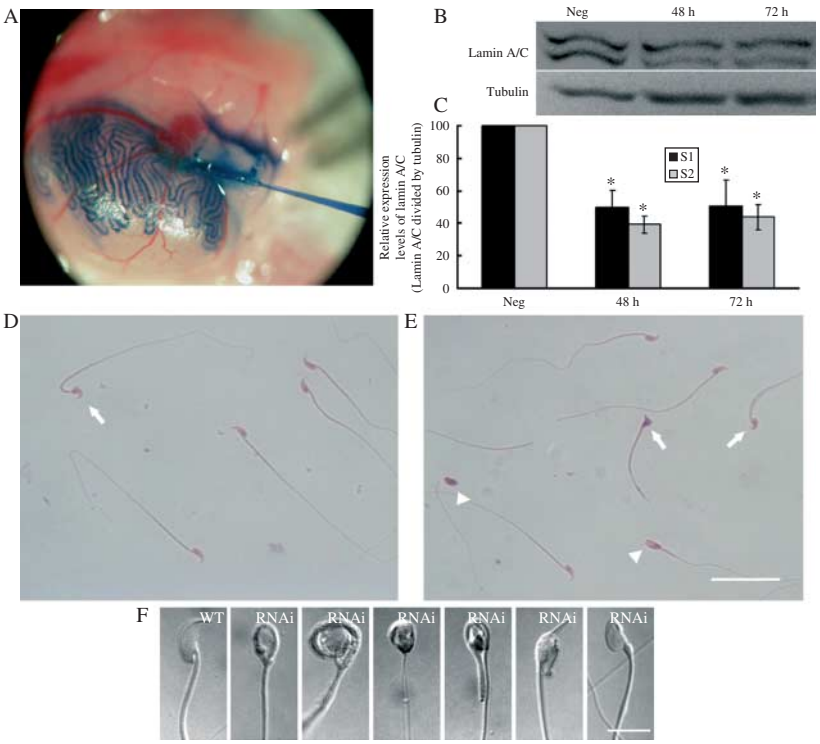

Figure 4 (A) Approximately, 30% of the seminiferous tubules in 3-week-old mouse testes were injected with siRNAs or negative control mixed with indicator (blue). (B) Western blotting analysis and statistical analysis (C) show efficiencies of lamin A/C siRNA *in vivo* 48 and 72 h after injection. β-tubulin was used as the loading control. S1 and S2 indicated lamin A and C respectively. Data represent a mean of triplicate experiments, and values are firstly normalized to loading tubulin control, and then expressed as percentage normalized to the negative control (100%). Significant differences compared with negative controls were also shown. **P* value <0.05 by Student's *t*-test. (D and E) The shapes of sperm from the caudal epididymis of mouse testis treated with the negative control (D) or siRNA (E). Arrows indicate abnormal sperm (bar = 20 μm). (F) Sperm collected from testes treated with siRNA showed round or irregular ball-like heads and not the typical hook-shaped head formation observed in controls (WT).

various developmental phases in mouse sperm. The co-localization with PSA and F-actin indicated that lamin A/C was a component of the acroplaxome, suggesting that it plays an important role in spermiogenesis. There was signal in the principal piece of the sperm tail of both F-actin and lamin A/C, the existence of F-actin in the tail is consistent with previous studies (Brener *et al.* 2003). However, the negative controls of lamin A/C also showed the signal existed in the sperm tail, we consider the tail distribution lamin A/C signal in epididymis sperm as nonspecific.

To the best of our knowledge, there was no transcription or translation of lamin A/C during spermiogenesis as this period is typically characterized by the replacement of histones by protamines (Steger 2001, Grimes 2004). Once the siRNA went into the spermatids to degrade the target mRNA, these cells were no longer able to increase the transcription of new mRNA in response. The subsequent decline in protein levels of the target gene could be maintained for a relative long period of time. We therefore chose to investigate haploid spermatids to achieve the maximum interference effect. The western blotting results confirmed that direct injection of siRNA into the seminiferous tubules through the rete testis was an ideal methodology to obtain the desired interference.

Approximately, 33% of the spermatozoa from siRNA-treated mice showed abnormal morphology. Interestingly, ∼28% of treated sperm had head defects, while this was rarely seen in the negative-control groups. These abnormal sperm heads lacked the typical hook-like appearance and also showed malformations in the acrosome and nucleus. Similar abnormalities have been seen in globozoospermia, a human disease characterized by round-headed sperm with deformed nuclei, abnormal acrosome, and malformed mitochondrial sheaths (Dam *et al.* 2007).

The mechanism leading to the formation of the sperm head is complicated. In normal elongating spermatids, the acrosome is tightly anchored to nucleus via the acroplaxome plate, subjacent to the perinuclear ring of the manchette, which has recently been structurally and biochemically characterized in the rat (Kierszenbaum *et al.* 2003, Toshimori & Ito 2003). It has been proposed that the combination of endogenous modulating mechanisms that are dependent on the acrosome–acroplaxome–manchette complex, along with exogenous contractile forces generated by F-actin-containing hoops, may play a co-operative role in shaping the head of spermatids (Kierszenbaum *et al.* 2003, 2004).

Recent research has provided molecular evidence for the relationship between the acrosome–acroplaxome–manchette complex and the shaping of round-headed sperm in humans. The phenotypes resembling globozoospermia were observed in *Agfg1* (*Hrb*), *Gopc,* and *Pick1* knockout mice (Kang-Decker *et al.* 2001, Yao *et al.* 2002, Xiao *et al.* 2009), providing further evidence of the importance of acrosomal formation for proper head shape in spermatids. The acroplaxome and manchette have also been shown to be important for the

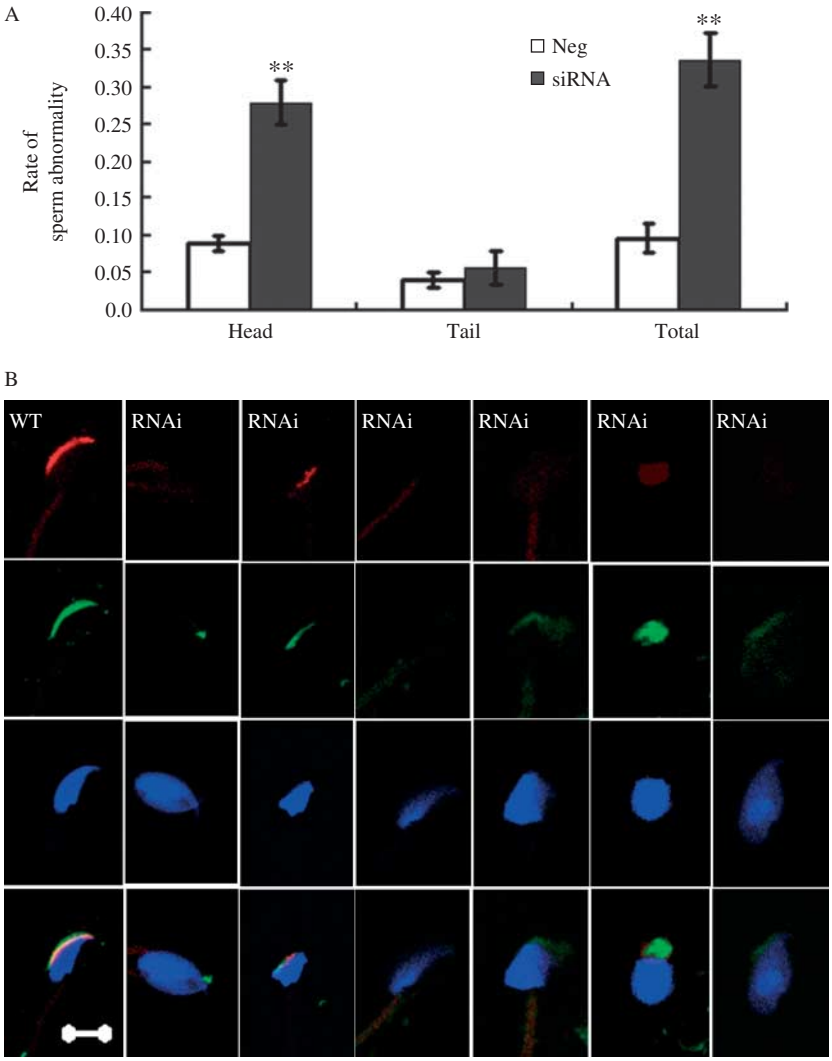

Figure 5 Effect of *in vivo* siRNA on sperm morphology in the caudal epididymis. Abnormalities in sperm were counted under light microscopy 3 weeks after injection and compared. (A) The rate of total sperm abnormality and head abnormality were significantly increased in the experimental group. Data represent a mean of triplicate experiments and significant differences are indicated by $^{**}P<0.01$. (B) Triple immunostaining of lamin A/C (red), PSA (green), and the nucleus by Hoechst (blue) for siRNA-treated and nontreated controls (WT) (bar = 5 μm).

development of head shape in spermatids. In the *Agfg1* mutant, the acroplaxome is compromised and may not be able to withstand the tension incurred during nuclear shaping in spermatids, resulting in globozoospermia (Kang-Decker *et al.* 2001). The disruption of *Hook1*, considered to be essential for the manchette development and function, resulted in ectopic positioning of the manchette in spermatids and produced the *Azh*

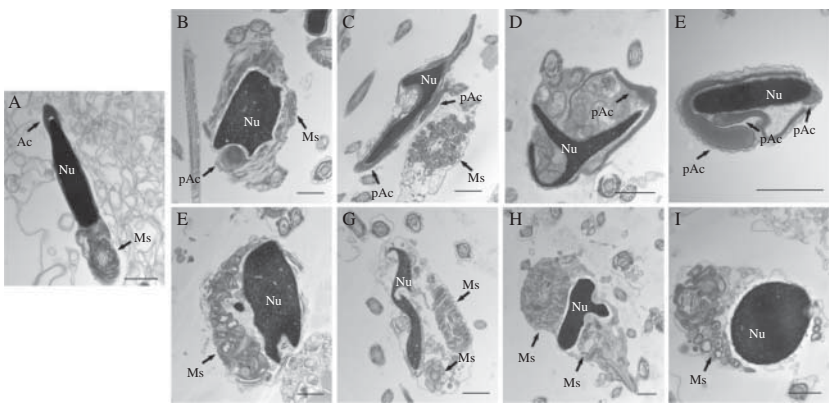

Figure 6 (A) Control spermatozoa nucleus and a flat, cap-like acrosome. (B, C, D, and E) Sperm with several discrete pseudoacrosome vesicles. (F, G, H, and I) Sperm nucleus with no acrosome and an abnormal arrangement of mitochondria in the mitochondrial sheath. Pseudoacrosome and abnormal mitochondrial sheaths are marked with arrows (bar = 1 μm, Nu, nucleus; Ms, mitochondrial sheath; pAc, pseudoacrosome).

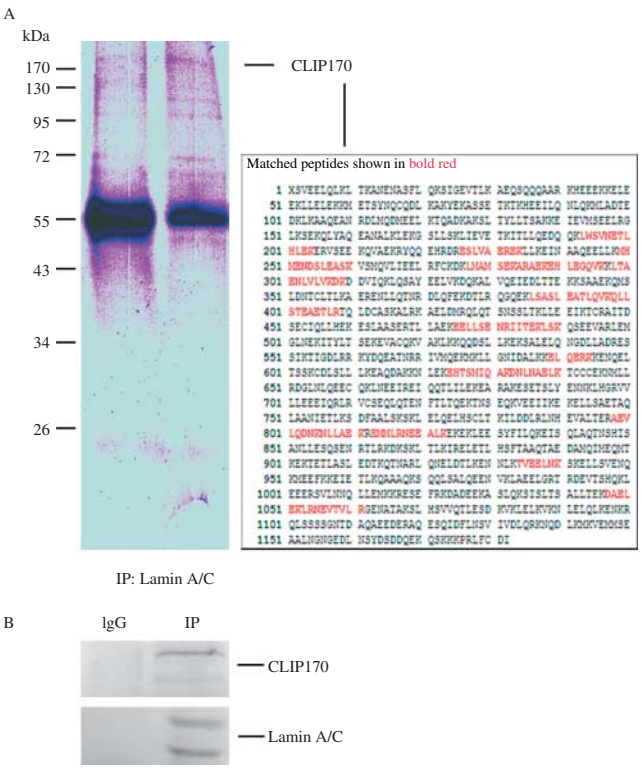

Figure 7 (A) Purification and identification of proteins associated with lamin A/C. Protein extracts of mouse testes were immunoprecipitated with normal rabbit IgG (lane 1) and anti-lamin A/C antibody (lane 2). The immunoprecipitated proteins were separated by SDS–PAGE and visualized by Coomassie Brilliant Blue (G250) staining. The protein co-purified with lamin A/C was identified as CLIP170 by mass spectrometric analysis. The paired CLIP170 peptides are shown in red. (B) Co-immunoprecipitation of endogenous lamin A/C and CLIP170, separated by SDS–PAGE and blotted with anti-CLIP170 antibody (upper panel) and lamin A/C were coimmunoprecipitated by CLIP170 specifically (lower panel). Normal rabbit IgG was used as the control.

phenotype, characterized by abnormal head shape (Cole *et al.* 1988). Abnormal spermatozoa were also observed in the RIM-BP3 knock-out, a protein that was shown to associate with the mouse manchette (Zhou *et al.* 2009). These data suggest that the acrosome, acroplaxome, and manchette, do not work independently, but as the acrosome–acroplaxome–manchette complex does influence spermatid head shape.

In this study, following the knockdown of the *Lmna* gene activity via intratesticular injection of siRNAs, the decrease in lamin A/C proteins led to a deficiency in assembling the acroplaxome and disturbed the formation of the manchette. We predict that the Golgi-derived proacrosomal vesicles were still able to fuse to form sacs; however, they were not able to anchor to the proper nuclear location in spermatids to generate the typical crescent moon-shaped acrosome and led to the abnormal acroplaxome. Thus, as we reported herein, the acrosome of these spermatozoa are deformed and fragmented. In addition, the deficient pseudoacrosome–acroplaxome–manchette complex was not able to withstand the tension during formation and therefore hampered the delicate balance between the exogenous force and endogenous clutch. We propose that these perturbations in the acrosome–acroplaxome–manchette complex resulted in the observed malformations in heads and acrosomes of spermatids.

In the current investigation, we characterized lamin A/C as a component of the acroplaxome and showed that it interacted with CLIP170, which was detected conspicuously on the manchette and the manchette ring of spermatids in WT mice (Akhmanova *et al.* 2005). *Clip170* male knock-out mice have been previously shown to be subfertile and produce sperm with abnormal heads (Akhmanova *et al.* 2005). Although in this study we did not present the direct interaction between lamin A/C and CLIP170, the similar sperm abnormalities have been observed following both decreased expression of LMNA and deficiencies of CLIP170 in knockouts. Hence it has been suggested that the two factors may act together to influence sperm development. Further exploration of the detailed interaction between lamin A/C and CLIP170 will help to elucidate the formation of mouse spermatid acroplaxome.

In conclusion, our study suggests that lamin A/C proteins were associated with acroplaxome proteins, and were essential for proper head shape in mouse spermatids. Human male infertility has often been related with abnormal spermatozoa head shape; therefore, the human *LMNA* gene could serve as one candidate gene for teratozoospermia. Further investigations will focus on the relationship between lamin A/C proteins and human infertility.

Declaration of interest

The authors declare that there is no conflict of interest that could be perceived as prejudicing the impartiality of the research reported.

Funding

This work was supported by grants from the National Natural Science Foundation of China (31000637 to X Guo), the National Basic Research Program of China (973 Program) (No. 2011CB944301 to X Huang), the National Natural Science Foundation of China (81222006 to X Guo), and Qing Lan Project.

References

Akhmanova A, Mausset-Bonnefont AL, van Cappellen W, Keijzer N, Hoogenraad CC, Stepanova T, Drabek K, van der Wees J, Mommaas M, Onderwater J *et al.* 2005 The microtubule plus-end-tracking protein CLIP-170 associates with the spermatid manchette and is essential for spermatogenesis. *Genes and Development* **19** 2501–2515. (doi:10.1101/gad.344505)

Alsheimer M, Liebe B, Sewell L, Stewart CL, Scherthan H & Benavente R 2004 Disruption of spermatogenesis in mice lacking A-type lamins. *Journal of Cell Science* **117** 1173–1178. (doi:10.1242/jcs.00975)

Brener E, Rubinstein S, Cohen G, Shternall K, Rivlin J & Breitbart H 2003 Remodeling of the actin cytoskeleton during mammalian sperm capacitation and acrosome reaction. *Biology of Reproduction* **68** 837–845. (doi:10.1095/biolreprod.102.009233)

Cole A, Meistrich ML, Cherry LM & Trostle-Weige PK 1988 Nuclear and manchette development in spermatids of normal and azh/azh mutant mice. *Biology of Reproduction* **38** 385–401. (doi:10.1095/biolreprod38.2.385)

Collard JF, Senécal JL & Raymond Y 1992 Redistribution of nuclear lamin A is an early event associated with differentiation of human promyelocytic leukemia HL-60 cells. *Journal of Cell Science* **101** 657–670.

Dam AH, Feenstra I, Westphal JR, Ramos L, van Golde RJ & Kremer JA 2007 Globozoospermia revisited. *Human Reproduction Update* **13** 63–75. (doi:10.1093/humupd/dml047)

Davis RO & Gravance CG 1994 Consistency of sperm morphology classification methods. *Journal of Andrology* **15** 83–91. (doi:10.1002/j.1939-4640.1994.tb01690.x)

Eddy EM 2002 Male germ cell gene expression. *Recent Progress in Hormone Research* **57** 103–128. (doi:10.1210/rp.57.1.103)

Galiová G, Bártová E, Raska I, Krejcí J & Kozubek S 2008 Chromatin changes induced by lamin A/C deficiency and the histone deacetylase inhibitor trichostatin A. *European Journal of Cell Biology* **87** 291–303. (doi:10.1016/j.ejcb.2008.01.013)

Genschel J & Schmidt HH 2000 Mutations in the LMNA gene encoding lamin A/C. *Human Mutation* **16** 451–459. (doi:10.1002/1098-1004(200012)16:6<451::AID-HUMU1>3.0.CO;2-9)

Grimes SR 2004 Testis-specific transcriptional control. *Gene* **343** 11–22. (doi:10.1016/j.gene.2004.08.021)

Guo X, Zhao C, Wang F, Zhu Y, Cui Y, Zhou Z, Huo R & Sha J 2010*a* Investigation of human testis protein heterogeneity using 2-dimensional electrophoresis. *Journal of Andrology* **31** 419–429. (doi:10.2164/jandrol.109.007534)

Guo X, Shen J, Xia Z, Zhang R, Zhang P, Zhao C, Xing J, Chen L, Chen W, Lin M *et al.* 2010*b* Proteomic analysis of proteins involved in spermiogenesis in mouse. *Journal of Proteome Research* **9** 1246–1256. (doi:10.1021/pr900735k)

Guo X, Zhang P, Qi Y, Chen W, Chen X, Zhou Z & Sha J 2011 Proteomic analysis of male 4C germ cell proteins involved in mouse meiosis. *Proteomics* **11** 298–308. (doi:10.1002/pmic.200900726)

Huang XY & Sha JH 2011 Proteomics of spermatogenesis: from protein lists to understanding the regulation of male fertility and infertility. *Asian Journal of Andrology* **13** 18–23. (doi:10.1038/aja.2010.71)

Huang XY, Guo XJ, Shen J, Wang YF, Chen L, Xie J, Wang NL, Wang FQ, Zhao C, Huo R *et al.* 2008 Construction of a proteome profile and functional analysis of the proteins involved in the initiation of mouse spermatogenesis. *Journal of Proteome Research* **7** 3435–3446. (doi:10.1021/pr800179h)

Ikawa M, Tergaonkar V, Ogura A, Ogonuki N, Inoue K & Verma IM 2002 Restoration of spermatogenesis by lentiviral gene transfer: offspring from infertile mice. *PNAS* **99** 7524–7529. (doi:10.1073/pnas.072207299)

Kang-Decker N, Mantchev GT, Juneja SC, McNiven MA & van Deursen JM 2001 Lack of acrosome formation in Hrb-deficient mice. *Science* **294** 1531–1533. (doi:10.1126/science.1063665)

Kierszenbaum AL & Tres LL 2004 The acrosome–acroplaxome–manchette complex and the shaping of the spermatid head. *Archives of Histology and Cytology* **67** 271–284. (doi:10.1679/aohc.67.271)

Kierszenbaum AL, Rivkin E & Tres LL 2003 Acroplaxome, an F-actin-keratin-containing plate, anchors the acrosome to the nucleus during shaping of the spermatid head. *Molecular Biology of the Cell* **14** 4628–4640. (doi:10.1091/mbc.E03-04-02REF20=10.1091/mbc.E03-04-0226)

Kierszenbaum AL, Tres LL, Rivkin E, Kang-Decker N & van Deursen JM 2004 The acroplaxome is the docking site of Golgi-derived myosin Va/Rab27a/b- containing proacrosomal vesicles in wild-type and Hrb mutant mouse spermatids. *Biology of Reproduction* **70** 1400–1410. (doi:10.1095/biolreprod.103.025346)

Link J, Jahn D, Schmitt J, Göb E, Baar J, Ortega S, Benavente R & Alsheimer M 2013 The meiotic nuclear lamina regulates chromosome dynamics and promotes efficient homologous recombination in the mouse. *PLoS Genetics* **9** e1003261. (doi:10.1371/journal.pgen.1003261)

Liu M, Hu Z, Qi L, Wang J, Zhou T, Guo Y, Zeng Y, Zheng B, Wu Y, Zhang P *et al.* 2013 Scanning of novel cancer/testis proteins by human testis proteomic analysis. *Proteomics* **13** 1200–1210. (doi:10.1002/pmic.201200489)

Lu L, Lin M, Xu M, Zhou ZM & Sha JH 2006 Gene functional research using polyethylenimine-mediated gene transfection into mouse spermatogenic cells. *Asian Journal of Andrology* **8** 53–59. (doi:10.1111/j.1745-7262.2006.00089.x)

Qi Y, Jiang M, Yuan Y, Bi Y, Zheng B, Guo X, Huang X, Zhou Z & Sha J 2013 ADP-ribosylation factor-like 3, a manchette-associated protein, is essential for mouse spermiogenesis. *Molecular Human Reproduction* **19** 327–335. (doi:10.1093/molehr/gat001)

Sha J, Zhou Z, Li J, Yin L, Yang H, Hu G, Luo M, Chan HC, Zhou K & Spermatogenesis study group 2002 Identification of testis development and spermatogenesis-related genes in human and mouse testes using cDNA arrays. *Molecular Human Reproduction* **8** 511–517. (doi:10.1093/molehr/8.6.511)

Steger K 2001 Haploid spermatids exhibit translationally repressed mRNAs. *Anatomica Embryologica* **203** 323–334. (doi:10.1007/s004290100176)

Toshimori K & Ito C 2003 Formation and organization of the mammalian sperm head. *Archives of Histology and Cytology* **66** 383–396. (doi:10.1679/aohc.66.383)

Wang L, Zhu YF, Guo XJ, Huo R, Ma X, Lin M, Zhou ZM & Sha JH 2005 A two-dimensional electrophoresis reference map of human ovary. *Journal of Molecular Medicine* **83** 812–821. (doi:10.1007/s00109-005-0676-y)

Wang G, Guo Y, Zhou T, Shi X, Yu J, Yang Y, Wu Y, Wang J, Liu M, Chen X *et al.* 2013 In-depth proteomic analysis of the human sperm reveals complex protein compositions. *Journal of Proteomics* **79** 114–122. (doi:10.1016/j.jprot.2012.12.008)

Worman HJ & Courvalin JC 2004 How do mutations in lamins A and C cause disease? *Journal of Clinical Investigation* **113** 349–351. (doi:10.1172/JCI200420832)

Worman HJ & Courvalin JC 2005 Nuclear envelope, nuclear lamina, and inherited disease. *International Review of Cytology* **246** 231–279. (doi:10.1016/S0074-7696(05)46006-4)

Xiao N, Kam C, Shen C, Jin W, Wang J, Lee KM, Jiang L & Xia J 2009 PICK1 deficiency causes male infertility in mice by disrupting acrosome formation. *Journal of Clinical Investigation* **119** 802–812. (doi:10.1172/JCI36230)

Yao R, Ito C, Natsume Y, Sugitani Y, Yamanaka H, Kuretake S, Yanagida K, Sato A, Toshimori K & Noda T 2002 Lack of acrosome formation in mice lacking a Golgi protein, GOPC. *PNAS* **99** 11211–11216. (doi:10.1073/pnas.162027899)

Zhou J, Du YR, Qin WH, Hu YG, Huang YN, Bao L, Han D, Mansouri A & Xu GL 2009 RIM-BP3 is a manchette-associated protein essential for spermiogenesis. *Development* **13** 373–382. (doi:10.1242/dev.030858)

Zhu YF, Cui YG, Guo XJ, Wang L, Bi Y, Hu YQ, Zhao X, Liu Q, Huo R, Lin M *et al.* 2006 Proteomic analysis of effect of hyperthermia on spermatogenesis in adult male mice. *Journal of Proteome Research* **5** 2217–2225. (doi:10.1021/pr0600733)

Received 9 January 2014
First decision 17 February 2014
Revised manuscript received 4 August 2014
Accepted 7 August 2014